Edelweiss Applied Science and Technology
ISSN: 2576-8484
Vol. 10, No. 1, 370-388
2026
Publisher: Learning Gate
DOI: 10.55214/2576-8484.v10i1.11616

Production of H_2-rich syngas and CO_2 capture from the steam gasification of human and animal derived bio-solids: Comparison with a valorization study for soil amendment

Despina Vamvuka[1*], Stelios Sfakiotakis[1], Konstantinos Kyriakidis[1], Ioannis Papakyriakopoulos[1]
[1]School of Mineral Resources Engineering, Technical University of Crete, Chania, Greece; dvamvouka@tuc.gr (D.V.).

Abstract: The steam gasification of human and animal-derived biosolids, integrated with CO_2 capture by a waste material, was investigated for the production of a H_2-rich syngas fuel. The potential of biochars to be used alternatively for soil amendment was also examined. A fixed-bed reactor/differential thermogravimetric-mass spectrometry system and column leaching were employed for the experiments, respectively. By sorbent addition, 86-87 % of CO_2 was captured, elevating the H_2 fraction in the generated gas by 80.1-104.5 % and the H_2/CO ratio up to 4-6 times. The gasification of animal bio-solid produced not only a higher yield of H_2, 3.1 m^3/kg, than human bio-solid, but also H_2 of higher purity, 84.3 mol%. When the biochars were leached through a quartzitic soil, some retention of nitrates occurred on the biochar's surface, while the release of phosphorus was negligible. The leachability of alkali cations, Ca, Mg, and K, was higher in the case of the animal biochar/soil system, whereas that of heavy metals was very low or practically null, supported by the neutral to alkaline pH of the leachates. Overall, the steam gasification of the bio-solids studied, in the presence of other wastes used as CO_2 sorbents, proved to be very advantageous. On the other hand, the application of biochars with composts or other wastes could improve soil amendment.

Keywords: *Bio-solids, CO_2 Capture, Soil Leaching, Steam Gasification.*

1. Introduction

The amounts of biosolids generated from human or animal wastewater treatment plants are very high and increase continuously, as a result of the growing global population and urbanization. Over 45 million dry tons of sewage sludge are produced annually worldwide [1], whereas swine sludge accounts for about 1 billion tons per year from China only [2]. The corresponding quantities produced by small countries, such as Greece, are approximately 30 kg per capita and 40 thousand tons [3], respectively.

Sewage or animal sludges contain several contaminants, such as parasites, bacteria, organic micro-pollutants, and heavy metals [4], rendering them potentially hazardous materials for human health and the entire ecosystem. Conventional management methods, such as landfilling or biological treatment, can cause not only environmental pollution and health problems but are also less cost-effective [5]. Furthermore, composting, if mismanaged, can cause contamination of soil and groundwater [6].

The high calorific value of dried biosolids, up to about 20 MJ/kg [6, 7], is challenging, making them promising renewable energy sources. Thus, Waste-to-Energy technologies have emerged as a viable alternative to traditional management methods, by reducing the volume of wastes and their adverse environmental impacts, while simultaneously producing energy and fuels. The gasification process offers the advantages of reduced pollutant emissions, higher efficiency, and the generation of a range of useful products, in comparison to incineration [8, 9].

When steam is used as the reactant gas, a syngas rich in hydrogen is produced, suitable for heat or power generation, as well as for the synthesis of transportation fuels and chemicals [4, 7, 9-11]. The

History: Received: 6 November 2025; Revised: 12 December 2025; Accepted: 16 December 2025; Published: 1 January 2026
* Correspondence: dvamvouka@tuc.gr

high moisture content of sewage or animal sludges can be eliminated through thermal drying with hot flue gases from the process, whereas the generated steam can be recycled to the steam gasification reactor. As such, the steam gasification process, using waste materials to produce hydrogen, can be considered a more economical pathway than the methane reforming process of natural gas [12]. The biochar generated from a pre-gasification step, having enhanced specific surface area and porosity compared to the raw material, can be alternatively utilized to adsorb various organic pollutants or heavy metals from soils and wastewaters, thus mitigating environmental risks, and/or to improve soil fertility by retaining plant nutrients and providing carbon in soils, thus contributing to carbon storage and sequestration [6, 13-15].

Several previous studies on the steam gasification of sewage sludge examined mixtures with horticultural waste, agricultural biomass, or corn stalks [11, 16, 17], focusing on synergistic effects, inherent alkali effects as catalysts, and self-moisture effects. The chemical kinetics of syngas generation have also been analyzed [12]. Catalysts such as activated carbon, sawdust biochar, dolomite, olivine, and limonite were used to reduce tar production [4, 7], resulting, however, in low syngas yields, up to 17%. CaO supported on Al_2O_3 was investigated as a CO_2 sorbent in fixed-bed reactor systems to enhance tar cracking and increase the H_2 volume fraction of the gas. Values between 73% and 83% H_2 at 650°C and 75% H_2 at 750°C with the addition of 5% CeO_2 were achieved [10], respectively. Unsupported lime, used at a CaO/sewage sludge ratio of 3:7, was found to produce 72% vol H_2 at 550°C during a two-stage fixed-bed process [18], whereas, at a ratio of 1:1, the H_2 content of the gas varied between 65.3% and 71% at 500-600°C, in another fixed-bed experimental study [19]. A maximum H_2 molar fraction of 50.8% was achieved during the steam gasification of sewage sludge in a moving-bed reactor, when a CaO-red mud/sewage sludge ratio of 30% was used at 750°C. At a temperature of 900°C, H_2 reached a value of 54.4% mol in the gas, and the syngas yield was 0.79 m^3/kg [11]. Concerning the steam gasification of swine sludge, there is a lack of literature data. A thermodynamic equilibrium model was developed to study the supercritical water gasification of pig manure only [2], indicating that decreasing the amount of pre-heating water, increasing the slurry concentration, and raising the temperature could enhance heat output and system efficiency.

Concerning the effects of sewage sludge biochar on the leaching of soil nutrients or heavy metals, some studies showed that the biochar produced at temperatures of 300-450°C had little effect on the retention of NO_3^- [20] or decreased the phosphorous concentration in plant roots [21] while the biochar produced at 500-700°C reduced the leaching of NH_4^+, NO_3^-, PO_4^{3-}, and K^+ in soil [20, 22, 23]. In addition, heavy metals were retained by the biochar [24], and the bioavailability of Cd, Pb, and Zn [25], as well as of Co and Cr [26], was greatly reduced. Field trials showed that the contents of these metals in soil increased gradually as the application of sewage sludge biochar increased from 7 t/ha to 30 t/ha, suggesting a safe application at < 15 t/ha [15]. Also, under field conditions, it was reported that over five years, sewage sludge biochar increased total N and Mehlich-1 P in the soil. A combination of mineral fertilizers provided all the macronutrients required for plant growth [26]. Finally, the persistence and bioavailability of polyaromatic hydrocarbons in sewage sludge biochar-amended soils were found to be related to the chemical properties of the soils, whereas a reduction of polyaromatic hydrocarbons was observed in acidic and neutral soils [27].

Relevant to the utilization of swine sludge biochar for soil amendment, previous research has focused on the co-application of this waste with woody biochars such as rice husk, maize straw, corn straw, and cotton stems [14, 28, 29], or composts such as wood chips, straw, and municipal solid waste composts, including the authors [14, 28, 30]. Results on the retention of nutrients and heavy metals, bioavailability of organic contaminants, and fungi/bacteria accumulation were analyzed.

In view of the above discussion, the steam gasification of human-derived bio-solids, in combination with CO_2 capture for yielding higher H_2 concentrations and reducing greenhouse gas emissions, is very insufficient and limited to the use of lime as a sorbent, while the steam gasification of animal-derived bio-solids has not been investigated so far. The novel concept of the current study was to integrate this thermochemical conversion process for H_2-rich syngas production with carbon mitigation, through the

Edelweiss Applied Science and Technology
ISSN: 2576-8484
Vol. 10, No. 1: 370-388, 2026
DOI: 10.55214/2576-8484.v10i1.11616

use of a waste material abundantly generated from the building sector, supporting in this way circular economy goals, with concomitant environmental and economic benefits. Furthermore, despite past research on sewage sludge biochar for soil amendment, the great diversity of such hazardous wastes and the variable composition of the soils significantly affect the mobility of the various ions, and the utilization of swine sludge biochar is limited to its co-application with composts or biomass. Accordingly, another aim of this study was to address these gaps and investigate the potential of these wastes to be used in agriculture.

For the steam gasification process, a fixed-bed reactor and TG-MS (thermogravimetric-mass spectrometry) system were employed. The feedstocks were characterized by physical, chemical, and mineralogical analyses. Fuel conversion, the composition of the gaseous products, their heating value, hydrogen yield, and energy recovery were determined at various temperatures and amounts of carbon dioxide sorbent used. Biochars admixed with a quartzitic soil were subjected to column leaching experiments, simulating field conditions. Important parameters were measured, and the leachability of nutrients and heavy metals was examined.

2. Materials and Methods

2.1. Elaboration of Raw Materials

The two waste materials investigated in this study were biosolids from the biological wastewater treatment units (BSH) in West Crete and from the biological waste treatment unit of Creta Farm swine breeding enterprise (BSS), also located in West Crete. Both sludges were undigested and received after the thickening and dewatering processes of the plants. Raw materials were air-dried, followed by grinding in a jaw crusher and a ball mill, and sieving to achieve a particle size of less than 500 μm.

A quartzitic soil, consisting of 55% sand, 45% silt, and 6% clay, was sampled according to the rectangular grid technique from the area of Chania in West Crete to be used for the leaching experiments of the BSH and BSS biochar materials. The soil was sieved to a particle size below 2 mm.

For the adsorption of CO_2 produced during the gasification tests, a fine powder with particle size less than 90 μm, generated as waste from concrete mortar production (WCF), was provided by the private corporation Finomix AE. The material was calcined at 950 °C in air so that its high calcite content was converted to lime. Subsequently, it was kept in a water-saturated environment within a sealed quartz vessel for about 10 days to transform lime into the active form of CO_2 sorbent, $Ca(OH)_2$ [31].

2.2. Physical and Chemical Characterization of Raw Materials

BSH and BSS materials were characterized in compliance with CEN/TC335 European Standards for the analysis of moisture, volatile components, fixed carbon, C, H, N, S, O levels, and calorific value. Physical characterization was performed in accordance with the Brunauer-Emmett-Teller (BET) method, utilizing a Quantachrome analyzer, model Autosorb 1Q-C-MP. Out-gassing of samples prior to the measurements occurred at 200 °C under vacuum. Chemical characterization was carried out by the Fourier-Transform Infrared Spectrometry technique (FTIR), using a PerkinElmer spectrophotometer, model Spectrum 100.

Crystalline mineral phases of BSH and BSS ashes, soil, and WCF materials were detected and identified by X-ray diffractometry integrated with Crystallography Open Database and DIFFRAC Plus software, utilizing a Bruker AXS equipment, model D8 Advance XRD. Major inorganic elements were determined through X-ray fluorescence spectrometry (XRF), by adopting a Bruker AXS spectrometer type S2 Ranger/EDS, whereas trace inorganic elements were derived by inductively coupled plasma mass spectrometry (ICP-MS), coupled with an Anton Paar Multiwave 3000 oven, using an Agilent Technologies apparatus, model ICP-MS 7500 cx.

In the case of liquid samples collected after leaching through the soil, the pH was recorded using a Mettler pH-meter, type Toledo LE438, and the electrical conductivity (EC) was measured with a Hanna instrument, model EC215. The chemical oxygen demand (COD), nitrates, phosphates, and phenols in

Edelweiss Applied Science and Technology
ISSN: 2576-8484
Vol. 10, No. 1: 370-388, 2026
DOI: 10.55214/2576-8484.v10i1.11616

the liquid leachates were measured via UV-VIS spectrophotometry, utilizing a LaMotte analyzer, type Smart 3. The analysis of metals in the soil extracts was performed using the ICP-MS technique, as previously mentioned.

2.3. Experimental Procedure of Gasification Experiments

The experimental system, which was used to carry out the gasification tests, has been described in detail in a previous research report by the authors [32]. The principal parts of this system were a stainless steel fixed bed reactor, equipped with a Ni-Cr-Ni thermocouple, surrounded by a high-temperature furnace, a pure nitrogen cylinder, an automatic water syringe pump, an ice bath for condensable volatiles, a silica gel filter for gas drying, a gas syringe type Luer Lock, and a TG/DTG thermal analyzer of Perkin Elmer, integrated with a mass spectrometer MS of Baltzers for quantitative gas analysis.

Biochars of BSH and BSS were produced through pyrolysis in nitrogen (flow rate 200 mL/min) at a final temperature of 600°C and a holding time at this temperature of 0.5 h. The devolatilized samples were subjected to steam gasification under the following experimental conditions: furnace heat-up rate 10°C/min, final temperature 900°C, steam/biochar=3 [32], Ca/C molar ratio of 1 or 2 when adding WCF as a CO_2 sorbent, retention time 1 h, high purity argon of TG/DTG-MS system (flow rate 35 mL/min), transfer capillary line of gases to MS made of fused silica and heated to 200 °C and Quadstar 422 software. Replicate tests were undertaken to assess the reliability and repeatability of the results. The interpretation of the results included the molar distribution of gaseous products and their heating value, the molar hydrogen-to-carbon monoxide ratio, the syngas and hydrogen yields, the conversion of the solid feedstock, and the recovery of energy [33] from the generated gas.

2.4. Experimental Procedure of Soil Leaching Experiments

Soil and BSH or BSS biochars, produced at a final temperature of 350°C, to maintain essential elements for the amelioration of the soil, were mixed with soil at proportions of 1000/50 g, respectively, following typical agronomical applications [34]. After incubation for one month, the mixtures were packed into PVC columns (25x250 mm) and saturated with distilled water. Leaching was then initiated by adding an amount of distilled water equal to the average annual rainfall quantity on the island of Crete (650 mm), for a time period lasting three months, trying to simulate as closely as possible rainfall conditions. Liquid effluents were filtered through micropore membrane filters and stored in the refrigerator until analyzed.

3. Results and Discussion

3.1. Physical and Chemical Characteristics of Raw Materials and Pyrolysis Products

From Table 1, representing the proximate and ultimate analyses and the specific surface area of the raw fuels, it can be seen that both materials had elevated amounts of volatile matter and ash, but also a significant content of carbon. The calorific values were quite high, especially that of BSS, due to its lower oxygen and higher carbon concentrations than BSH fuel. Such values are comparable to or even greater than most low-rank coals. Concerning gaseous emissions during thermochemical processes, Table 1 shows that sulfur emissions are expected to be very low; however, those of nitrogenous species could be significant, probably in the form of gaseous ammonia from the gasification process. On the other hand, the high nitrogen content of these materials could be advantageous if they are applied to soils for plant nutrition.

The rate of evolution of light gases, with respect to temperature, during the devolatilization stage of the fuel up to 600°C, as derived by the TG/DTG-MS system, is illustrated in Figure 1, whereas the yield of each generated product, along with its associated higher heating value, is demonstrated in Figure 2. The main components of light gas were CO_2 and CO, which peaked at about 350°C and were associated with the thermal cracking of C-O and C=O bonds or carboxylic acids. Methane and light hydrocarbons were released in smaller amounts at higher temperatures, with their maxima located at

Edelweiss Applied Science and Technology
ISSN: 2576-8484
Vol. 10, No. 1: 370-388, 2026
DOI: 10.55214/2576-8484.v10i1.11616

450-550°C. The evolution of H_2, which is generated by the splitting of stronger aliphatic or aromatic bonds, started at a temperature of 500°C. The yields of light gas and solid char were higher in the case of BSS material, as Figure 2 shows. The higher heating value of gas-phase and liquid-phase by-products (BSHO and BSSO bio-oils) of the pyrolysis process was very high, ranging between 16.7-22.5 MJ/m^3 and 34-34.5 MJ/kg, respectively, implying their valuable energy support for the endothermic process studied. The heating value of the gas was calculated from the quantitative analysis performed through the TG/DTG system.

Table 1.
Proximate, ultimate analyses (% dry) and structural characteristics of raw materials.

Sample	Volatile Matter	Fixed Carbon	Ash	C	H	N	O	S	Higher Heating Value (MJ/kg)	Specific Surface Area (m²/g)
BSH	66.2	16.3	17.5	40.1	6.4	7.3	27.8	0.9	17.2	0.5
BSS	61.0	11.9	27.1	43.3	6.5	4.3	17.7	1.1	20.4	2.8

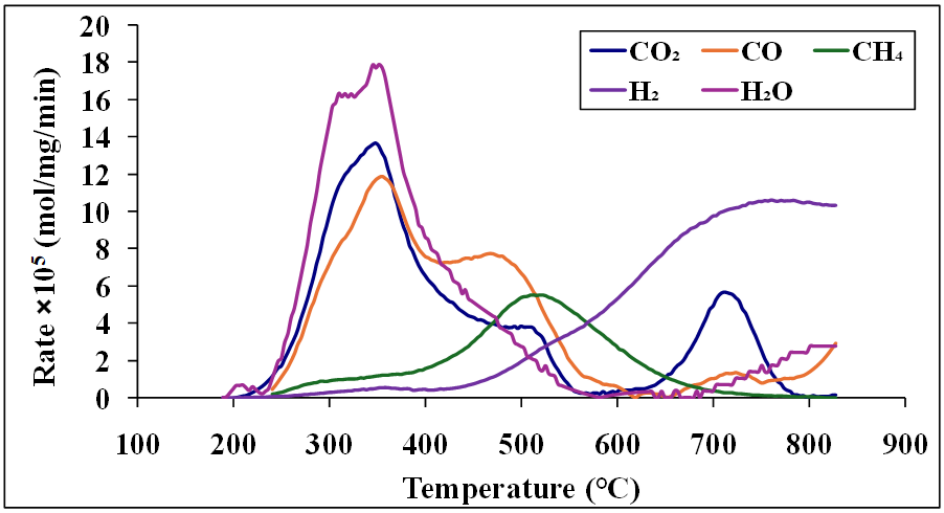

Figure 1.
Rate of evolution of light gases of BSS fuel during the pyrolysis stage.

Edelweiss Applied Science and Technology
ISSN: 2576-8484
Vol. 10, No. 1: 370-388, 2026
DOI: 10.55214/2576-8484.v10i1.11616

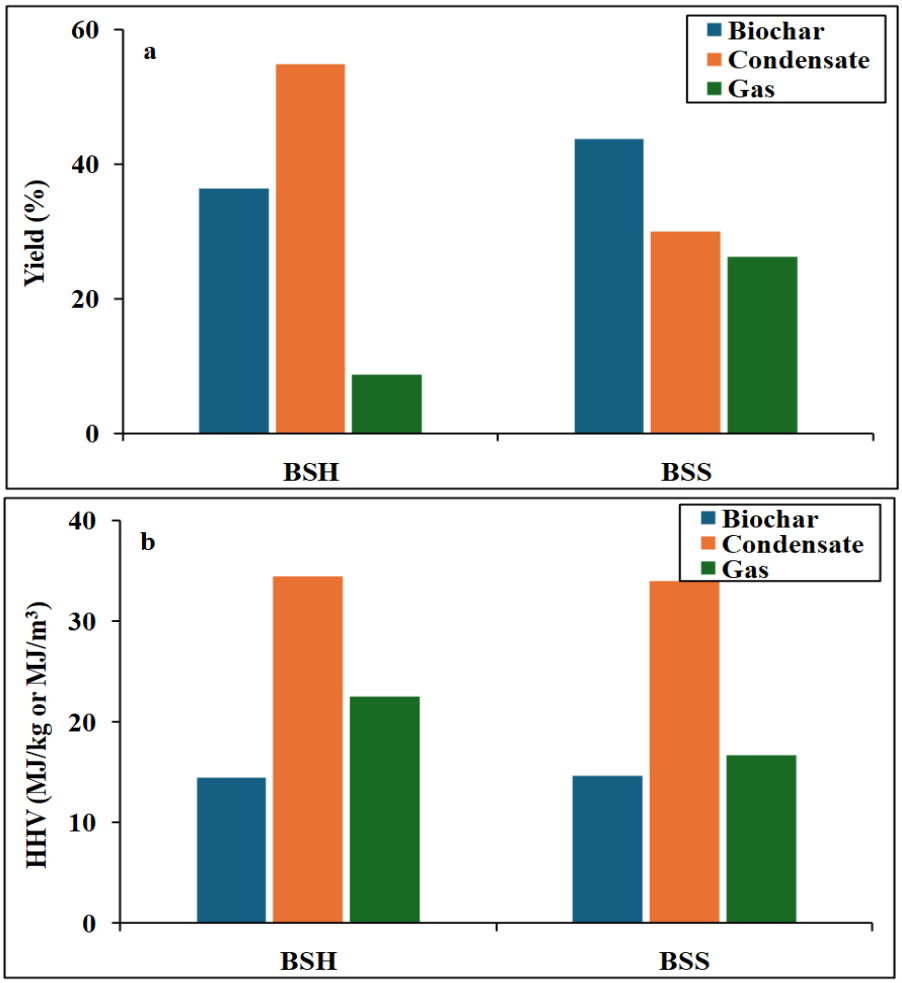

Figure 2.
Yield (a) and higher heating value (b) of pyrolysis products of BSH and BSS fuels.

MS unit. Biochars and bio-oils were subjected to CHNOS analysis (Table 2), and their heating value was derived using the following equations Vamvuka et al. [32]:

$$HHV_{bio-oil} = 0.3383C + 1.422(H - \frac{O}{8})(MJ/kg) \quad (1)$$

$$HHV_{biochar} = 33.5C + 142.3H - 15.4O - 14.5N) \times 10^{-2}(MJ/kg) \quad (2)$$

Furthermore, Table 2, which compares the physical and chemical traits of the solid and liquid products, deduced after the thermal treatment in a nitrogen atmosphere, shows that hydrogen and oxygen contents of the chars (BSHB, BSSB) were greatly reduced after emission of volatile compounds, pointing to the development of aromatic structures during the process and higher carbon stability [6, 20]. Also, the increase in fixed carbon of aromatic nature and in mineral matter of both chars is beneficial in the case of soil applications for carbon sequestration, resistance to microbial and chemical degradation, and enrichment of soils in organic matter and micronutrients [6]. However, the much greater amount of ash in the chars, compared to the raw feedstocks, resulted in a drop in calorific value. In relation to the chars' surface area-to-mass ratio, which is very important for their gasification reactivity or the adsorption of nutrients/pollutants, it can be seen from the above table that it was increased by 7 to 12 fold during the thermal treatment for the BSH and BSS materials, respectively.

Edelweiss Applied Science and Technology
ISSN: 2576-8484
Vol. 10, No. 1: 370-388, 2026
DOI: 10.55214/2576-8484.v10i1.11616

Nevertheless, the obtained values were quite low due to the high amount of ash in the chars, preventing the access of reactant gas, as well as the rather low pyrolysis temperature.

The FTIR spectra of BSH and BSS biochars are illustrated in Figure 3. In the case of BSH, the distinct peak at 948 cm^{-1} wave number corresponds to C=C bending of alkene compounds. The strong peak at 1084 cm^{-1} can be assigned to either C-O stretching vibrations in primary alcohols or stretching vibrations of C-N in amines. Another strong peak at 1546 cm^{-1}, characteristic of N-O stretching of nitro compounds, confirms the high nitrogen content of the char measured by the CHNOS analysis. The small peaks at 2332 cm^{-1} and 2356 cm^{-1} are attributed to O=C=O stretching from carbon dioxide, whereas the broad band at 3420 cm^{-1} represents stretching vibrations of O-H in alcohols. In the case of the BSS spectrum (Figure 3b), the peaks at 558 cm^{-1} and 572 cm^{-1} indicate stretching of C-X halocompounds, and the small peak at 874 cm^{-1} indicates C-H bending from substituted benzene derivatives. The strong peaks at 1028 cm^{-1} and 1424 cm^{-1} represent stretching vibrations of C-N in amines and bending vibrations of O-H in carboxylic acids, respectively. The small peak at 2364 cm^{-1} corresponds to the O=C=O stretching of carbon dioxide. Finally, the broad band at 3380 cm^{-1} is assigned to O-H stretching vibrations from alcohols and possibly to N-H stretching of amines.

The concentrations of major and trace elements in BSH and BSS biochars, along with those of the WCF material used as the CO_2 sorbent, are included in Table 3. BSH biochar presented elevated contents of Ca, Fe, and P, which are plant nutrients, and moderate contents of Si, Mg, and K. Higher amounts of Ca, P, and Mg were measured in the BSS biochar, typical for animal sludges [13]. Among the trace elements, Zn was present in considerable amounts in both chars, while Pb was only present in BSH char. However, all measured values are below the limits set for landfill disposal [35]. Concerning the WCF material, this consisted almost entirely of Ca. The XRD spectra, which are presented in the Appendix, indicated that the Ca in both chars was principally bound in quite soluble forms of carbonates and sulfates, such as calcite and anhydrite, while Fe, P, and Mg were mainly incorporated in insoluble whitlockite magnesian. Lower amounts of Fe and P were found in rodolicoite, whereas K was found in carbonate fairchildite. Upon application to soils, the solubility of the mineral phases containing such nutrient elements must be considered for their availability.

3.2. Performance of BSH and BSS Fuels during Steam Gasification

The influence of temperature on the composition of the resulting gas from the steam gasification of BSH and BSS chars is depicted in Figure 4. As observed, increasing the process temperature from 700 °C to 900 °C significantly affects the gas composition. The volume fractions of H_2 and CO_2 progressively increase with temperature, reaching peak values at 900 °C, 55.6 mol% H_2 and 24.1 mol% CO_2 for BSH fuel, and 64.5 mol% H_2 and 17.7 mol% CO_2 for BSS fuel. This trend is attributed to the endothermic nature of reactions (3) and (4), as well as the water-gas shift reaction (7), which becomes thermodynamically favorable at higher temperatures [36]. Conversely, the concentration of CO in the gas mixture decreased significantly as the temperature increased from 700 °C to 900 °C, reaching a minimum value of 18.2 mol% in the case of BSH char and 17 mol% in the case of BSS char.

Table 2.
Proximate, ultimate analyses (% dry) and structural characteristics of solid and liquid pyrolysis products.

Sample	Fixed Carbon	Ash	C	H	N	O	S	Higher Heating Value (MJ/kg)	Specific Surface Area (m^2/g)
BSHB	52.7	47.3	42.5	1.1	5.4	3.3	0.4	14.5	3.6
BSHO	-	-	69.5	9.1	9.7	11.1	0.6	34.5	-
BSSB	51.0	49.0	42.2	1.2	3.0	4.3	0.3	14.7	32.7
BSSO	-	-	69.1	8.9	9.9	11.6	0.5	34.0	-

Edelweiss Applied Science and Technology
ISSN: 2576-8484
Vol. 10, No. 1: 370-388, 2026
DOI: 10.55214/2576-8484.v10i1.11616

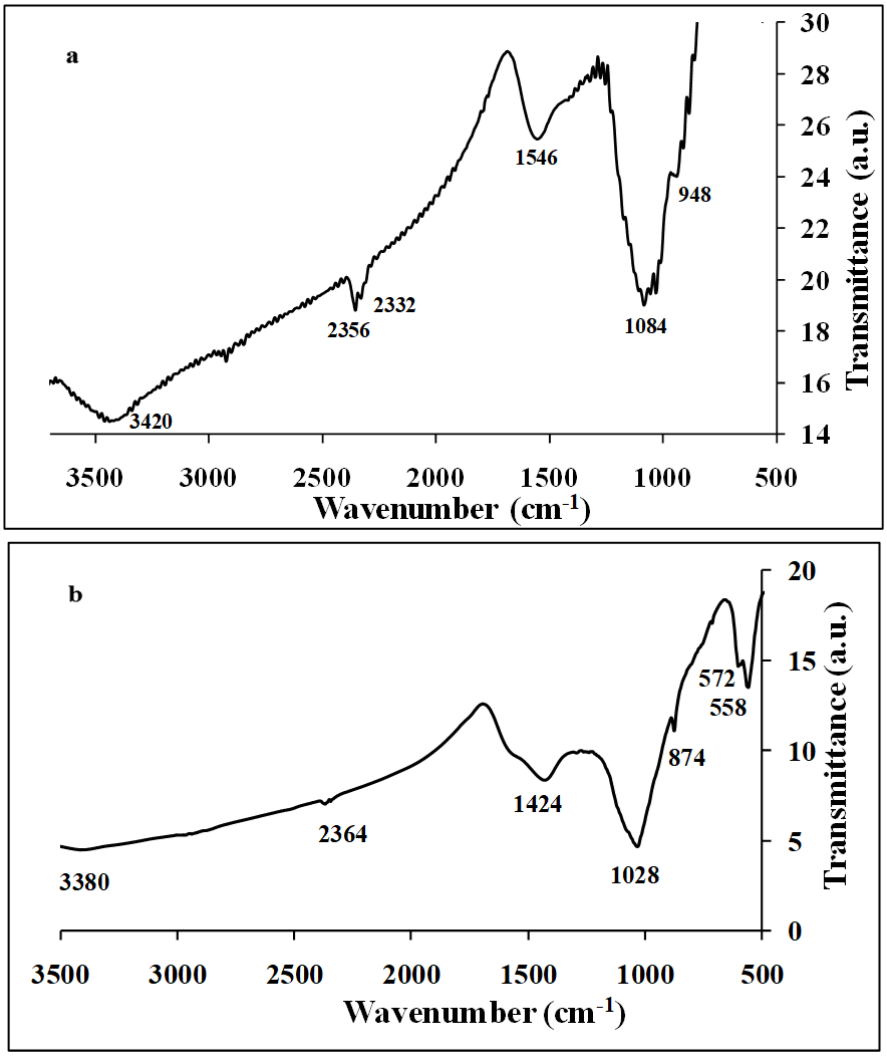

Figure 3.
FTIR spectra of (a) BSH and (b) BSS biochars.

This drop in CO content reveals that, although the Boudouard reaction (5) was promoted at higher temperatures, CO was consumed by reaction (7) and the reverse reaction (8). The small increase in CH_4 gas confirms its production through the reverse reaction (8), as reaction (6) needs elevated pressures to be favored. It should be mentioned that, although the concentrations of CxHy were not included in the graph due to scaling reasons, they were very low, between 0.02-0.1 mol%, whereas minor quantities of NH_3 were detected in the product gas, and extremely low quantities of H_2S. The elevation in H_2 generation from the steam gasification of these materials could also be attributed to the alkali (K, Na) or alkaline earth compounds (Ca, Mg) identified in the mineral matter, or hematite [11, 32], which are known to catalyze the process. Furthermore, the larger specific surface area of BSS char, as compared to BSH char, could explain its higher reactivity towards steam.

Edelweiss Applied Science and Technology
ISSN: 2576-8484
Vol. 10, No. 1: 370-388, 2026
DOI: 10.55214/2576-8484.v10i1.11616

Table 3.
Concentration of major and trace elements in biochars and sorbent materials.

Sample	Major Elements (g/kg)								Trace Elements (mg/kg)				
	Ca	Al	Si	Fe	Mg	K	Na	P	Cu	Zn	Cr	Pb	As
BSHB	38.5	6.9	22.5	31.0	13.3	18.3	2.5	39.7	236.8	822.9	45.8	51.9	9.9
BSSB	88.5	7.5	22.0	6.6	34.9	11.8	11.6	47.1	97.9	336.1	14.7	-	-
WCF	675.0	9.0	7.5	1.4	10.2	1.6	1.5	-					

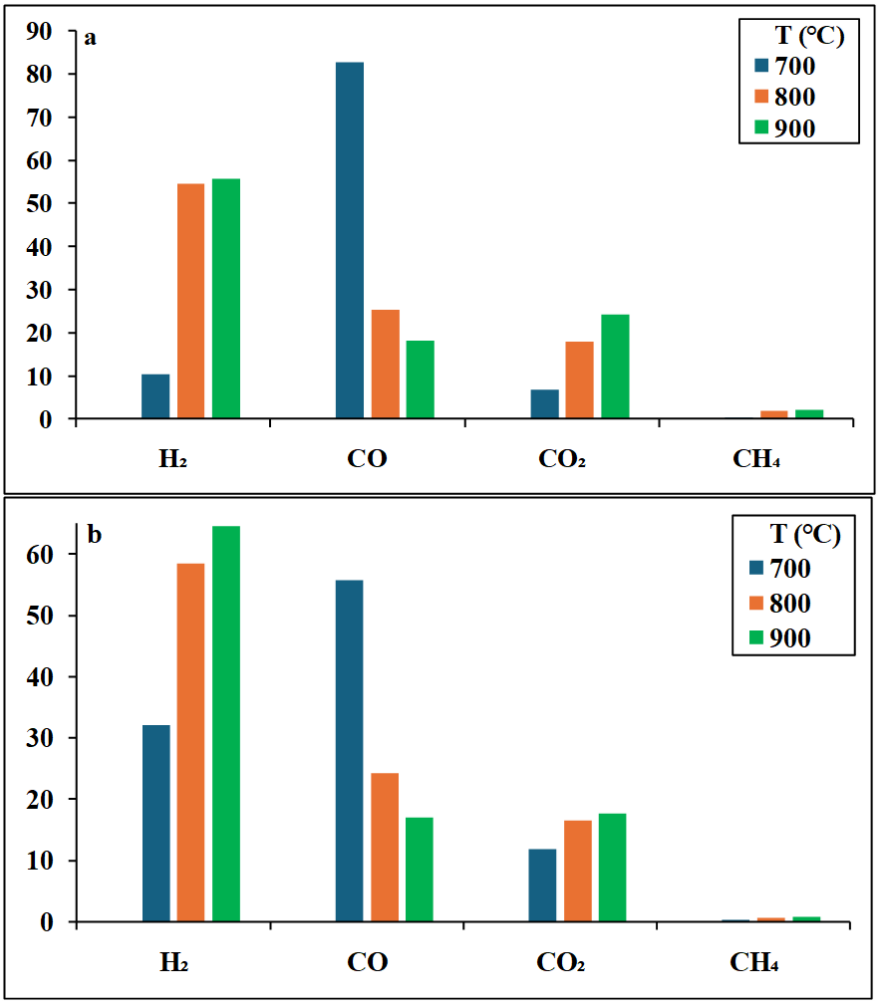

Figure 4.
Composition of gasification gas as a function of temperature for (a) BSH and (b) BSS chars.

$$C + H_2O \rightarrow CO + H_2 \quad (3)$$
$$C + 2H_2O \rightarrow CO_2 + 2H_2 \quad (4)$$
$$C + CO_2 \rightarrow 2CO \quad (5)$$
$$C + 2H_2 \rightarrow CH_4 \quad (6)$$
$$CO + H_2O \leftrightarrow CO_2 + H_2 \quad (7)$$
$$CH_4 + H_2O \leftrightarrow CO + 3H_2 \quad (8)$$

Edelweiss Applied Science and Technology
ISSN: 2576-8484
Vol. 10, No. 1: 370-388, 2026
DOI: 10.55214/2576-8484.v10i1.11616

When WCF was added to the reactor to capture the CO_2 produced, the final temperature was maintained at 750°C to inhibit the breakdown of $CaCO_3$, which would enrich the output gas in CO_2. As stated in the experimental section, the active CO_2 sorbent was $Ca(OH)_2$.

$$CaO + H_2O \rightarrow Ca(OH)_2 \quad (9)$$
$$Ca(OH)_2 + CO_2 \rightarrow CaCO_3 + H_2O \quad (10)$$

Indeed, portlandite was identified by the XRD analysis of WCF, as shown in the XRD spectrum in the Appendix. In practical applications, the heat for the calcination of sorbent $CaCO_3$ could be provided by the combustion of unconverted char, pyrolysis by-products, or a waste heat source. Figure 5 indicates the effect of the Ca/C molar ratio on the H_2/CO molar ratio and the higher heating value of the resultant gas. As can be seen, the presence of WCF material significantly elevated the H_2/CO ratio up to 4-6 times compared to tests without the addition of CO_2 sorbent. Maxima occurred at a Ca/C=2 (2.4 for BSH char and 6.7 for BSS char), suggesting that this process could be further utilized for the generation of biofuels and chemicals [37]. The higher heating value of the gas was also increased from approximately 11 MJ/m^3 at Ca/C=0 to 13.4 MJ/m^3, as shown in Figure 5b.

Table 4 presents the detailed distribution of gases in the final mixture at 750 °C and Ca/C=2, along with the fuel conversion (GE) and energy recovery (ERE) values. With the addition of WCF sorbent, 86-87% of CO_2 was captured, shifting the equilibrium towards the production of H_2, so that the H_2 fraction was elevated by 80.1-104.5% in the presence of WCF material, achieving a value of 67.9 mol% for BSH char and 84.3 mol% for BSS char. The continuous removal of CO_2 from the generated gas favored under these conditions reactions (3), (4), and (7) to the right, in contrast to the Boudouard reaction (5), which would barely take place at 750 °C. The increase in the CH_4 percentage of the gas mixture, when the CO_2 sorbent was added, suggests that the higher amount of syngas produced promoted the steam-methane reaction (8) to the left side. Moreover, Table 4 indicates that the carbon conversion of both fuels was complete. Thus, the high gas yield and its greater heating value, due to its enrichment in combustible gases H_2, CO, and CH_4, resulted in particularly high energy recovery from the gasification process.

Current results on H_2 concentration of product gas are comparable to those reported in the literature or even higher, considering that no catalysts were used in this study. For instance, approximately 75 mol% H_2 was generated from the steam conversion of sewage sludge to gas at 750 °C, using CaO/Al_2O_3 as a CO_2 sorbent and 5% CeO_2 as a catalyst [10]. Also, a two-stage fixed bed process, using a CaO/sewage sludge ratio of 1:1, found that the H_2 content of the gas varied between 65.3 mol% and 71 mol% at 500-600°C, according to another experimental study [19]. When 30% red mud was added to the CaO sorbent, the maximum H_2 molar fraction achieved at 750°C was 50.8% [11]. Unfortunately, no literature data is available for comparison relevant to the steam gasification of swine sludge, to the authors' knowledge, under similar conditions to the present work.

Table 4.
Gasification performance of the fuels at 750°C and molar Ca/C=2.

Sample	Composition of gas (mol%)					HHV (MJ/m^3)	GE (%)	ERE
	H_2	CO_2	CO	CH_4	C_xH_y			
BSHB	67.9	1.2	28.0	2.8	0.04	13.4	100	2.2
BSSB	84.3	2.1	12.5	1.1	0.02	12.8	100	3.2

Edelweiss Applied Science and Technology
ISSN: 2576-8484
Vol. 10, No. 1: 370-388, 2026
DOI: 10.55214/2576-8484.v10i1.11616

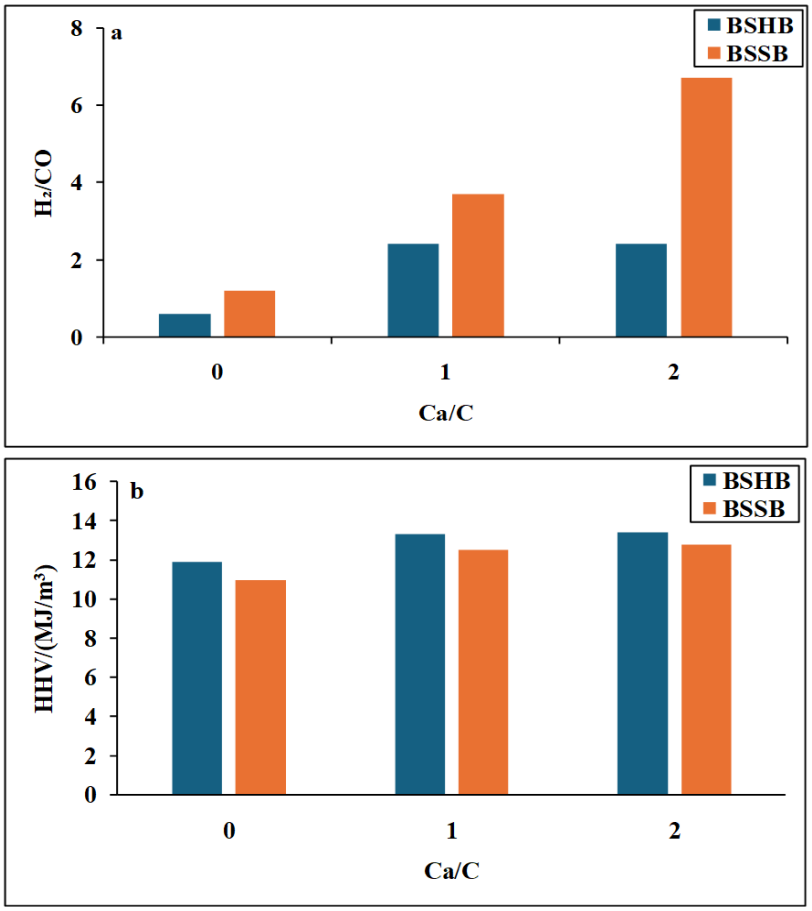

Figure 5.
Effect of Ca/C molar ratio on (a) H_2/CO molar ratio and (b) the higher heating value of resultant gas at 750°C.

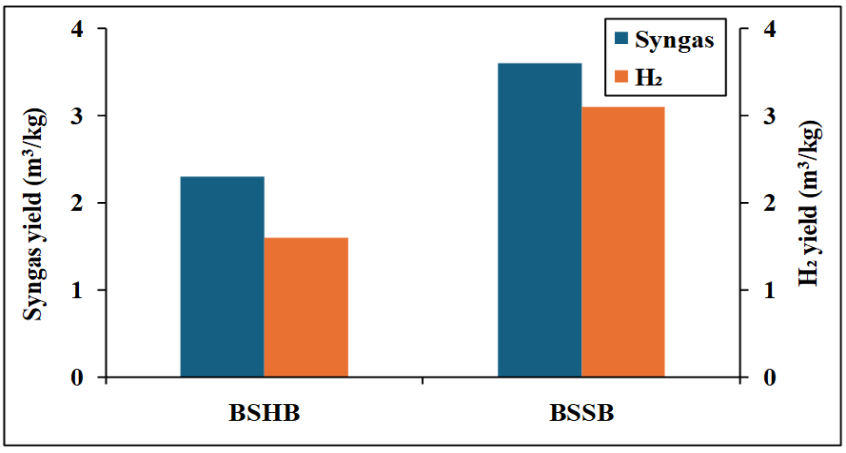

Figure 6.
Syngas and hydrogen yields of resultant gas at 750°C and Ca/C=2.

Perhaps the most important outcome when trying to convert waste biomass materials to biofuels is the syngas or H_2 yield. Figure 6 compares the performance of the two fuels, in terms of syngas and H_2

Edelweiss Applied Science and Technology
ISSN: 2576-8484
Vol. 10, No. 1: 370-388, 2026
DOI: 10.55214/2576-8484.v10i1.11616

yield, for the optimum Ca/C molar ratio of 2 at 750°C. As clearly seen, the significant reduction of CO_2 emissions achieved was reflected in the syngas yield, which was far higher (2.3-3.6 m^3/kg char) than previously reported values in the literature [11, 18]. The results show that upon addition of WCF sorbent, the steam gasification of BSS waste material generated not only a higher yield of H_2 (3.1 m^3/kg char) than BSH material but also H_2 of higher purity (84.3 mol%), as previously discussed (Table 4).

3.3. Leaching Behavior of BSH and BSS Biochars through the Soil

The concentrations of COD, NO_3^-, PO_4^{3-}, and phenols as a function of leaching time, along with the pH and EC values, measured in the liquid extracts from the column leaching experiments from the BSHB/soil and BSSB/soil mixtures, are summarized in Table 5. As can be seen, the pH of the BSHB/soil sample increased from 7 to 7.9 over time, while for the BSSB/soil sample, the trend was opposite, and pH decreased from 8.1 to 7.2 after a period of 90 days. This behavior can be explained by the higher amount of carbonates in BSH biochar, as shown above from the XRD spectra, in the form of calcite and fairchildite, which could have been partly dissolved in water during the experiments. The electrical conductivity was low for both solid mixtures, thus favoring the availability of nutrients through the soil. The COD value measured from the sewage sludge (BSH) biochar was negligible. On the other hand, the one corresponding to the animal sludge (BSS) biochar was quite high at the beginning of the tests; however, it gradually dropped by threefold at the end of the 90-day period. It is possible that the carboxylic and alcoholic compounds, identified by the FTIR spectrum of BSS biochar, adsorbed some organic species from the soil during the tests on biochar's surface [8]. Nevertheless, COD values were lower than previous literature data for manures derived from other waste sludge materials [8, 30].

The release of nitrates in the leachates was similar for the two samples and decreased over time, indicating some retention of these ions on the surface of the biochars, which could be beneficial for soils and plants by enabling a slower uptake of nitrogen from biochar application. Regarding phosphate ion release in the extracts, Table 5 shows that no such ions were leached from the BSHB/soil mixture, as phosphorus was incorporated into insoluble whitlockite magnesian mineral, as previously discussed. The small amount of phosphates measured in the BSSB/soil extracts is most likely due to the hydroxylapatite mineral, detected in the XRD spectrum of BSS biochar. Therefore, the availability of phosphorus to agricultural soils from these materials would be negligible. Nonetheless, the amount of phenols leached was very low. The retention of nitrate and phosphate ions by various biochars applied to soils and the enhancement of nitrogen and phosphorus uptake by plants have also been reported in other studies [20-22, 24].

Table 5.
Characteristic leaching parameters of biochars through the soil.

Sample	Leaching Time (days)					
	1	**8**	**22**	**36**	**60**	**90**
BSHB/Soil						
pH	7.0	7.2	7.5	7.7	7.9	7.9
EC (mS/cm)	0.8	0.7	0.6	0.4	0.2	0.2
COD (mg/L)	49.0	-	-	-	-	-
NO_3^- (mg/L)	35.0	32.0	31.0	29.0	24.0	20.0
PO_4^{3-} (mg/L)	-	-	-	-	-	-
Phenols (mg/L)						0.64
BSSB/Soil						
pH	8.1	8.0	7.6	7.4	7.3	7.2
EC (mS/cm)	2.7	0.9	0.9	0.8	0.7	0.5
COD (mg/L)	660.0	347.0	305.0	273.0	232.0	215.0
NO_3^- (mg/L)	46.0	44.0	37.0	33.0	26.0	21.0
PO_4^{3-} (mg/L)	7.0	30.0	32.0	35.0	36.0	39.0
Phenols (mg/L)						1.7

Edelweiss Applied Science and Technology
ISSN: 2576-8484
Vol. 10, No. 1: 370-388, 2026
DOI: 10.55214/2576-8484.v10i1.11616

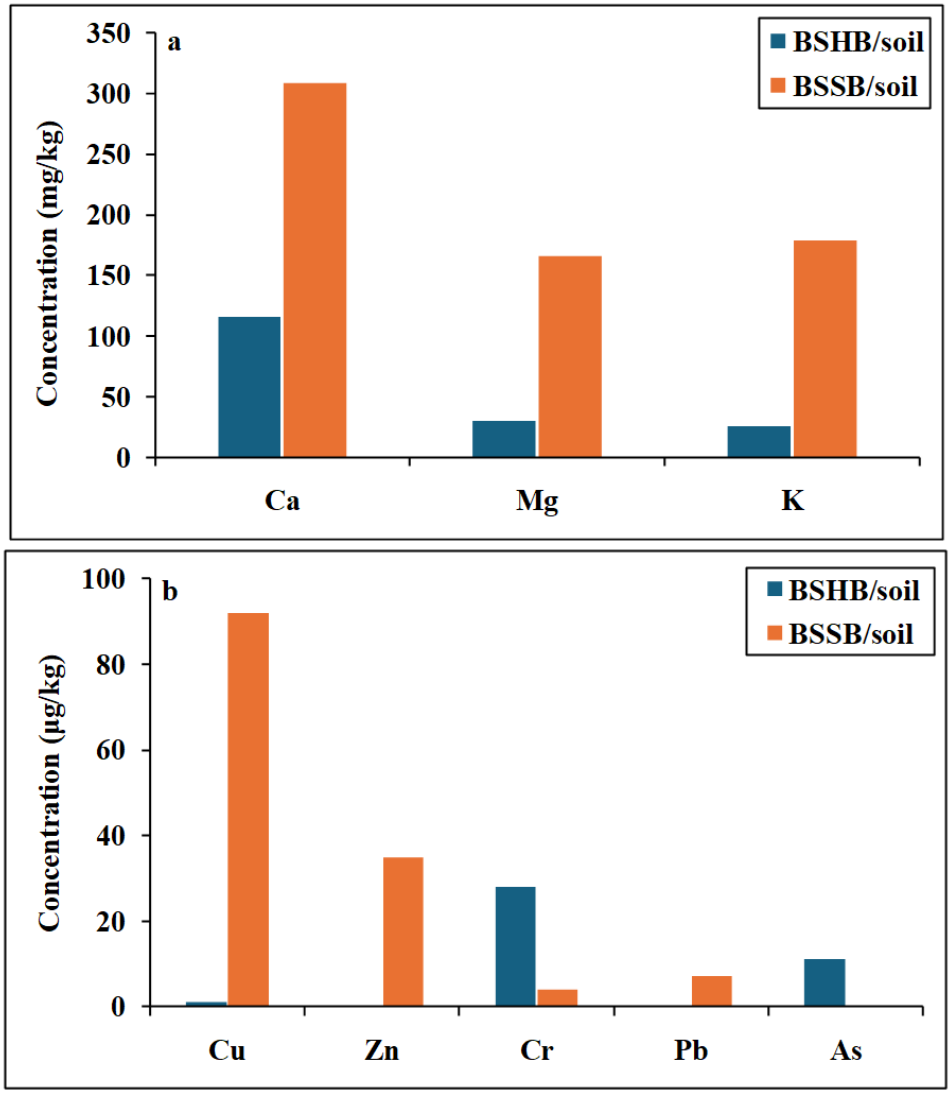

Figure 7.
Cumulative concentration of (a) major and (b) trace elements in the leachates.

The cumulative concentration of the most mobile major and trace elements, determined in the leachates of BSHB/soil and BSSB/soil mixtures from the column tests, is illustrated in Figure 7. As can be noticed, only Ca was extracted from BSH biochar in moderate amounts, due to the soluble forms of calcite and anhydrite, according to the XRD spectra. The higher leachability of alkali cations Ca and Mg from the BSSB/soil sample is attributed to the increased amount of these metals in BSS biochar compared to BSH biochar, as well as the partial solubility of hydroxylapatite and dolomite identified by XRD analysis. The increased migration of K from the BSSB/soil system could be assigned to the soluble sylvite mineral present in this biochar. Concerning trace elements, Figure 7 indicates that their cumulative concentration in the liquid effluents from both samples was very low and well below allowable limits for deposition in landfills [35]. Toxic metals Pb and As were not quantified at all in the leachates corresponding to BSHB/soil and BSSB/soil mixtures, respectively. The low leachability of these heavy metals through the soil could be influenced by many factors, among which are the chemical and mineralogical composition of both biochars and soil, and system pH. Heavy metals could be retained

Edelweiss Applied Science and Technology
ISSN: 2576-8484
Vol. 10, No. 1: 370-388, 2026
DOI: 10.55214/2576-8484.v10i1.11616

by the solid materials through complexation, electrostatic attraction, competition between elements, etc., or could be bound in stable phosphates, aluminosilicates, or oxides present in the biochar/soil systems [20, 30, 38]. Furthermore, the neutral to alkaline pH measured during the tests contributed to the low mobility of these elements through the soil. These results are in agreement with other studies [23, 25, 26, 30] where the leachability of heavy metals to the soils from similar biochar materials was found to be very low.

4. Conclusions

The thermal treatment of BSH and BSS materials increased the aromatic nature of the chars and their mineral matter, which was enriched in Ca, P, Fe, and Mg. Liquid and gaseous by-products, possessing high heating values up to 34.5 MJ/kg and 22.5 MJ/m^3, respectively, could offer valuable energy for the endothermic processes studied.

When the biochars were gasified by steam up to 900°C, the H_2 content in the product gas varied between 55.6 mol% and 64.5 mol%, whereas that of CO_2 varied between 17.7 mol% and 24.1 mol%. With the addition of WCF sorbent, 86-87% of CO_2 was captured, elevating the H_2 fraction in the generated gas by 80.1-104.5% and increasing the H_2/CO ratio to 4-6 times. The gasification of BSS waste material produced not only a higher yield of H_2, 3.1 m^3/kg, than BSH material, but also H_2 of higher purity, 84.3 mol%.

When the biochars were leached through a quartzitic soil, the COD values dropped significantly after a 90-day period, the release of nitrates decreased with time, implying some retention of these ions on the biochar's surface, while the release of phosphorus was negligible, due to its binding in insoluble whitlockite magnesian mineral. The leachability of alkali cations, Ca, Mg, and K, was higher in the case of the BSSB/soil system, whereas that of heavy metals was very low or practically null, supported by the neutral to alkaline pH of the leachates.

In alignment with eco-friendly waste management within a circular economy framework, the steam gasification of BSH and BSS materials, in the presence of other wastes used as CO_2 sorbents, proved to be very advantageous. On the other hand, application of these biochars with composts or other wastes could improve soil amendment by retaining toxic heavy metals or nutrients of high extractability.

Transparency:

The authors confirm that the manuscript is an honest, accurate, and transparent account of the study; that no vital features of the study have been omitted; and that any discrepancies from the study as planned have been explained. This study followed all ethical practices during writing.

Acknowledgments:

The authors kindly thank the laboratories of Hydrocarbons Chemistry, Applied Mineralogy, Geochemistry, Quality Control, Health and Safety in the Mineral Industry, Hydrogeochemical Engineering, and Soil Remediation of the Technical University of Crete and the Institute of Chemical Engineering Sciences in Patras for the various analyses of the samples.

References

[1] Y. Huang, M. Chen, and Q. Li, "Decentralized drying-gasification scheme of sewage sludge with torrefied biomass as auxiliary feedstock," *International Journal of Hydrogen Energy*, vol. 45, no. 46, pp. 24263-24274, 2020. https://doi.org/10.1016/j.ijhydene.2020.06.036

[2] Y. Wang *et al.*, "Thermodynamic and environmental analysis of heat supply in pig manure supercritical water gasification system," *Energy*, vol. 263, p. 125694, 2023.

[3] European Parliament and Council, "Directive 2009/28/EC on the promotion of the use of energy from renewable sources and amending and subsequently repealing Directives 2001/77/EC and 2003/30/EC," *Official Journal of the European Union, L*, vol. 140, pp. 16–62, 2009.

[4] B. S. Kang *et al.*, "Valorization of sewage sludge via air/steam gasification using activated carbon and biochar as catalysts," *International Journal of Hydrogen Energy*, vol. 54, pp. 284-293, 2024. https://doi.org/10.1016/j.ijhydene.2023.04.188

[5] A. Ghirardini, V. Grillini, and P. Verlicchi, "A review of the occurrence of selected micropollutants and microorganisms in different raw and treated manure–environmental risk due to antibiotics after application to soil," *Science of the Total Environment*, vol. 707, p. 136118, 2020. https://doi.org/10.1016/j.scitotenv.2019.136118

[6] D. Vamvuka, S. Sfakiotakis, and O. Pantelaki, "Evaluation of gaseous and solid products from the pyrolysis of waste biomass blends for energetic and environmental applications," *Fuel*, vol. 236, pp. 574-582, 2019.

[7] D. Alper, E. Babayiğit, G. E. Zengin, H. C. Okutan, and A. Sarıoğlan, "The catalytic influence of low-cost natural minerals on sewage sludge gasification for hydrogen production," *International Journal of Hydrogen Energy*, vol. 142, pp. 966-980, 2025. https://doi.org/10.1016/j.ijhydene.2025.03.009

[8] X. Yang *et al.*, "Sorption-enhanced thermochemical conversion of sewage sludge to syngas with intensified carbon utilization," *Applied Energy*, vol. 254, p. 113663, 2019.

[9] S. Moles, I. Martinez, M. S. Callén, J. Gómez, J. M. López, and R. Murillo, "Pilot-scale study of sorption-enhanced gasification of sewage sludge," *Fuel*, vol. 360, p. 130611, 2024.

[10] S. Chen *et al.*, "Hydrogen-rich syngas production via sorption-enhanced steam gasification of sewage sludge," *Biomass and Bioenergy*, vol. 138, p. 105607, 2020. https://doi.org/10.1016/j.biombioe.2020.105607

[11] Y. Cheng, Z. Guo, R. Hong, N. Chen, and R. Han, "Enhanced production of hydrogen-rich gas from municipal sewage sludge gasification using a CaO-RM composite catalyst," *International Journal of Hydrogen Energy*, vol. 77, pp. 824-833, 2024.

[12] U. Lee, J. Dong, and J. Chung, "Experimental investigation of sewage sludge solid waste conversion to syngas using high temperature steam gasification," *Energy Conversion and Management*, vol. 158, pp. 430-436, 2018.

[13] D. Vamvuka, S. Dermitzakis, D. Pentari, and S. Sfakiotakis, "Valorization of meat and bone meal through pyrolysis for soil amendment or lead adsorption from wastewaters," *Food and Bioproducts Processing*, vol. 109, pp. 148-157, 2018. https://doi.org/10.1016/j.fbp.2018.04.002

[14] L. Xiang *et al.*, "Biochar combined with compost to reduce the mobility, bioavailability and plant uptake of 2, 2', 4, 4'-tetrabrominated diphenyl ether in soil," *Journal of Hazardous Materials*, vol. 374, pp. 341-348, 2019.

[15] P. Zhang, X. Zhang, X. Yuan, R. Xie, and L. Han, "Characteristics, adsorption behaviors, Cu (II) adsorption mechanisms by cow manure biochar derived at various pyrolysis temperatures," *Bioresource Technology*, vol. 331, p. 125013, 2021. https://doi.org/10.1016/j.biortech.2021.125013

[16] Q. Hu, Y. Dai, and C.-H. Wang, "Steam co-gasification of horticultural waste and sewage sludge: Product distribution, synergistic analysis and optimization," *Bioresource Technology*, vol. 301, p. 122780, 2020. https://doi.org/10.1016/j.biortech.2020.122780

[17] G. Kong *et al.*, "Tunable H2/CO syngas production from co-gasification integrated with steam reforming of sewage sludge and agricultural biomass: A experimental study," *Applied Energy*, vol. 342, p. 121195, 2023.

[18] X. Yang *et al.*, "Tunable syngas production from two-stage sorption-enhanced steam gasification of sewage sludge," *Chemical Engineering Journal*, vol. 404, p. 126069, 2021.

[19] D. Lin, W. Kai, X. Xie, A. Kozlov, M. Penzik, and B. Li, "Steam gasification of lime dried sewage sludge: Effects of temperature and addition of lime," *Fuel*, vol. 371, p. 131932, 2024. https://doi.org/10.1016/j.fuel.2024.131932

[20] H. Yuan, T. Lu, Y. Wang, Y. Chen, and T. Lei, "Sewage sludge biochar: Nutrient composition and its effect on the leaching of soil nutrients," *Geoderma*, vol. 267, pp. 17-23, 2016.

[21] R. A. Rehman *et al.*, "Efficiency of various sewage sludges and their biochars in improving selected soil properties and growth of wheat (Triticum aestivum)," *Journal of Environmental Management*, vol. 223, pp. 607-613, 2018.

[22] P. Mbasabire, Y. T. Murindangabo, J. Frouz, and J. Brom, "Characterization, fractionation and untapped potential of phosphate-amended sewage sludge biochar in soil-plant systems," *Chemosphere*, vol. 367, p. 143565, 2024. https://doi.org/10.1016/j.chemosphere.2024.143565

[23] J. F. Lustosa Filho, R. d. S. R. Viana, L. C. A. Melo, and C. C. de Figueiredo, "Changes in phosphorus due to pyrolysis and in the soil-plant system amended with sewage sludge biochar compared to conventional P fertilizers: A global meta-analysis," *Chemosphere*, vol. 371, p. 144055, 2025. https://doi.org/10.1016/j.chemosphere.2024.144055

[24] C. C. de Figueiredo, J. K. M. Chagas, J. da Silva, and J. Paz-Ferreiro, "Short-term effects of a sewage sludge biochar amendment on total and available heavy metal content of a tropical soil," *Geoderma*, vol. 344, pp. 31-39, 2019.

[25] E. S. Penido, G. C. Martins, T. B. M. Mendes, L. C. A. Melo, I. do Rosário Guimarães, and L. R. G. Guilherme, "Combining biochar and sewage sludge for immobilization of heavy metals in mining soils," *Ecotoxicology and Environmental Safety*, vol. 172, pp. 326-333, 2019. https://doi.org/10.1016/j.ecoenv.2019.01.110

[26] J. K. M. Chagas, C. C. de Figueiredo, and J. Paz-Ferreiro, "Sewage sludge biochars effects on corn response and nutrition and on soil properties in a 5-yr field experiment," *Geoderma*, vol. 401, p. 115323, 2021.

[27] M. Kończak, P. Godlewska, M. Wiśniewska, and P. Oleszczuk, "Chemical properties of soil determine the persistence and bioavailability of polycyclic aromatic hydrocarbons in sewage sludge-or sewage sludge/biomass-derived biochar-amended soils," *Environmental Pollution*, vol. 319, p. 120909, 2023.

[28] J. Liang *et al.*, "Changes in heavy metal mobility and availability from contaminated wetland soil remediated with combined biochar-compost," *Chemosphere*, vol. 181, pp. 281-288, 2017. https://doi.org/10.1016/j.chemosphere.2017.04.081

[29] X. Wei *et al.*, "Biochar addition for accelerating bioleaching of heavy metals from swine manure and reserving the nutrients," *Science of the Total Environment*, vol. 631, pp. 1553-1559, 2018.

[30] D. Vamvuka and K. Esser, "Experimental study on the effectiveness of an untreated animal sludge biochar to release/retain nutrients and heavy metals from soil amended with compost," *Materials International*, vol. 2, pp. 242–249, 2020.

[31] X. Zeng *et al.*, "Enhanced hydrogen production by the catalytic alkaline thermal gasification of cellulose with Ni/Fe dual-functional CaO based catalysts," *International Journal of Hydrogen Energy*, vol. 46, no. 65, pp. 32783-32799, 2021. https://doi.org/10.1016/j.ijhydene.2021.07.142

[32] D. Vamvuka, E. Afthentopoulos, and S. Sfakiotakis, "H2-rich gas production from steam gasification of a winery waste and its blends with industrial wastes. Effect of operating parameters on gas quality and efficiency," *Renewable Energy*, vol. 197, pp. 1224-1232, 2022. https://doi.org/10.1016/j.renene.2022.07.162

[33] D. Vamvuka, S. Sfakiotakis, and M. Galetakis, "Catalytic co-gasification of refuse derived fuel and industrial waste biomass under steam using a novel waste material as CO2 sorbent," *International Journal of Innovative Science, Engineering and Technology*, vol. 12, pp. 4–14, 2025.

[34] S. Jeffery, F. G. Verheijen, M. van der Velde, and A. C. Bastos, "A quantitative review of the effects of biochar application to soils on crop productivity using meta-analysis," *Agriculture, Ecosystems & Environment*, vol. 144, no. 1, pp. 175-187, 2011. https://doi.org/10.1016/j.agee.2011.08.015

[35] European Biochar Certificate (EBC), *Guidelines for a sustainable production of biochar (Version 10.5E)*. Frick, Switzerland: Carbon Standards International, 2025.

[36] S. U. Ilyas, T. Sultan, N. A. Merdad, and M. Shahbaz, "Thermal conversion of oil and sewage sludge via gasification and pyrolysis into H2-Rich syngas and pyrolysis products with CO2 capture: Equilibrium modelling," *International Journal of Hydrogen Energy*, vol. 172, p. 151328, 2025. https://doi.org/10.1016/j.ijhydene.2025.151328

[37] G. Nagy and Z. Dobó, "Experimental investigation of fixed-bed pyrolysis and steam gasification of food waste blended with woody biomass," *Biomass and Bioenergy*, vol. 139, p. 105580, 2020. https://doi.org/10.1016/j.biombioe.2020.105580

[38] H. R. Boostani, M. Najafi-Ghiri, A. G. Hardie, and D. Khalili, "Comparison of Pb stabilization in a contaminated calcareous soil by application of vermicompost and sheep manure and their biochars produced at two temperatures," *Applied Geochemistry*, vol. 102, pp. 121-128, 2019. https://doi.org/10.1016/j.apgeochem.2019.01.013

Appendix

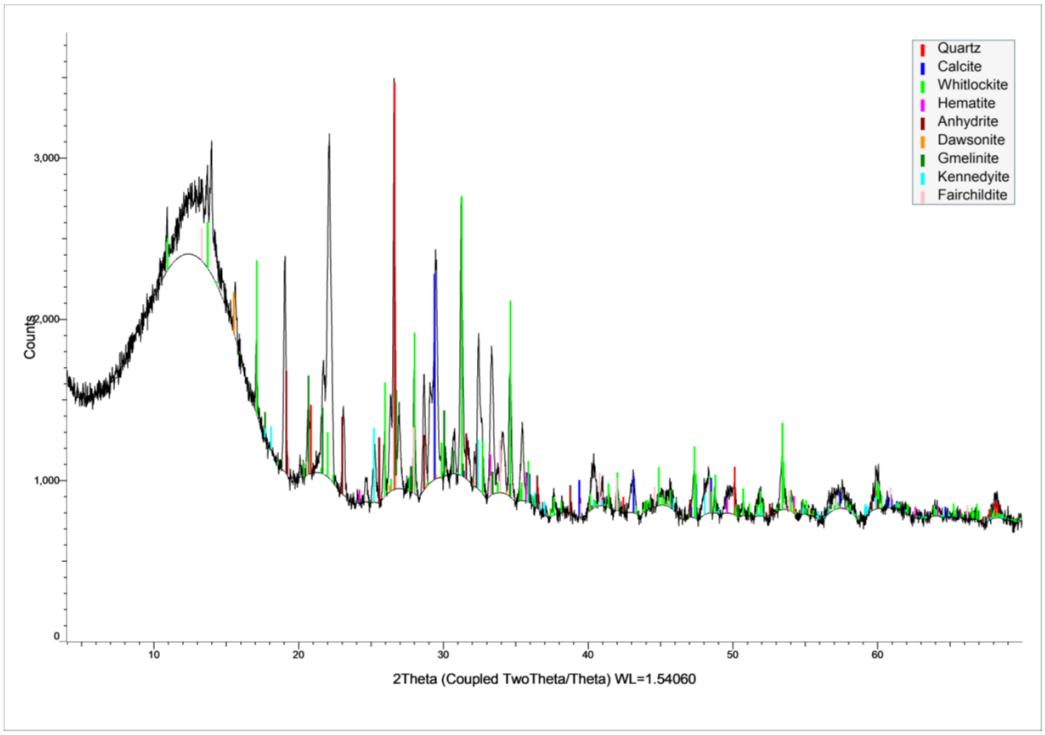

(a)

Edelweiss Applied Science and Technology
ISSN: 2576-8484
Vol. 10, No. 1: 370-388, 2026
DOI: 10.55214/2576-8484.v10i1.11616

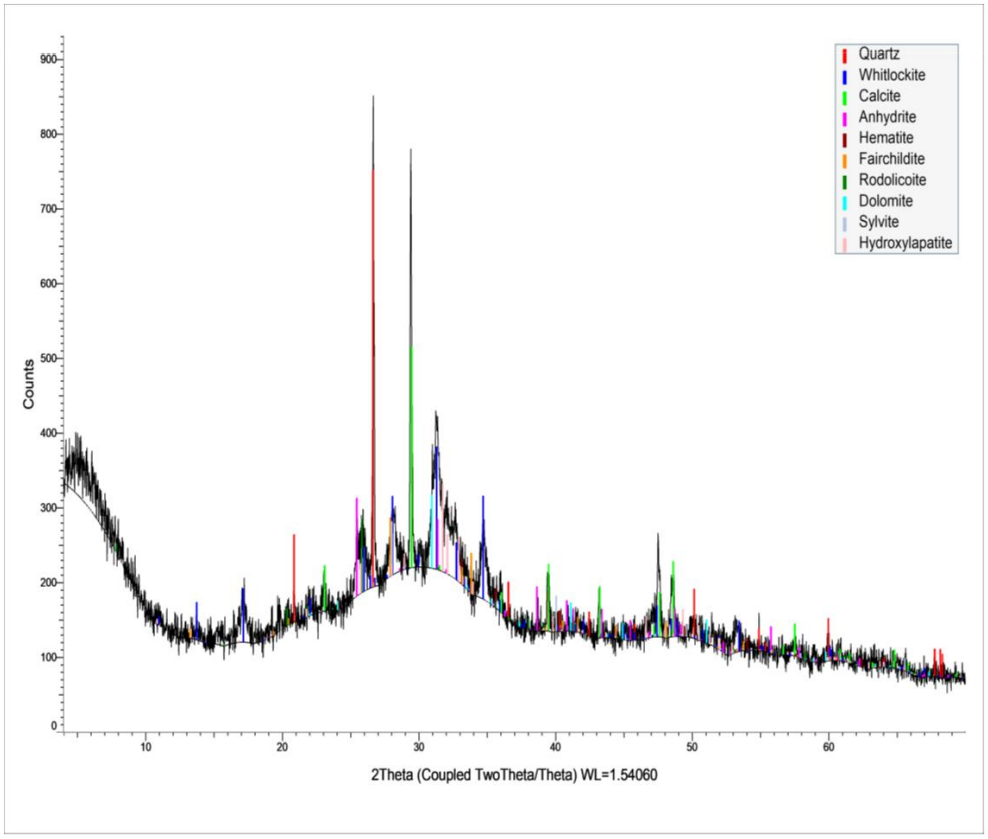

(b)

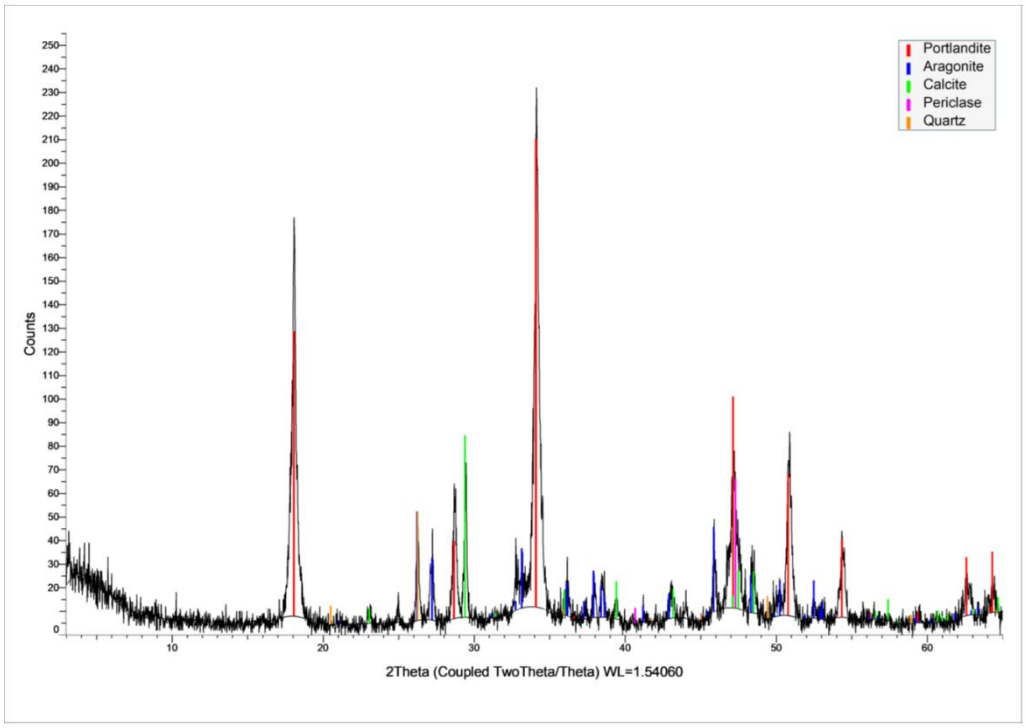

(c)

Edelweiss Applied Science and Technology
ISSN: 2576-8484
Vol. 10, No. 1: 370-388, 2026
***DOI**: 10.55214/2576-8484.v10i1.11616*

(d)

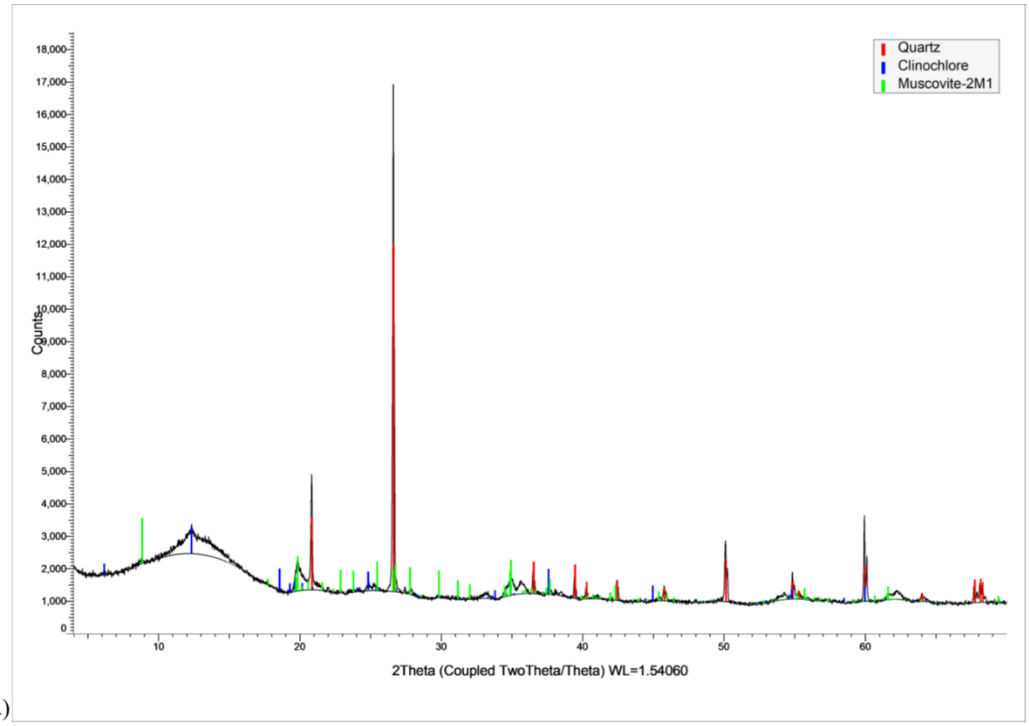

Figure A1.
XRD spectra of (a) BSH ash, (b) BSS ash, (c) WCF sorbent, and (d) soil.

Edelweiss Applied Science and Technology
ISSN: 2576-8484
Vol. 10, No. 1: 370-388, 2026
DOI: 10.55214/2576-8484.v10i1.11616